

**Carbon Nanotubes Coated with Diamond Nanocrystals and Silicon Carbide  
by Hot-filament Chemical Vapor Deposition below 200° C substrate temperature**

F.Piazza<sup>1\*</sup>, G. Morell<sup>2,3</sup>, J. Beltran Huarac<sup>2,3</sup>, G. Paredes<sup>1</sup>, M. Ahmadi<sup>2</sup>, M. Guinel<sup>2,3,4</sup>

<sup>1</sup>Nanoscience Research Laboratory, Pontificia Universidad Católica Madre y Maestra, Autopista Duarte km 1 1/2, Apartado Postal 822, Santiago, Dominican Republic

<sup>2</sup>Department of Physics, University of Puerto Rico, San Juan, PR 00936, USA

<sup>3</sup>Institute for Functional Nanomaterials, University of Puerto Rico, San Juan, PR 00931, USA

<sup>4</sup>Department of Chemistry, University of Puerto Rico, San Juan, PR 00936, USA

**Abstract**

Multi-walled carbon nanotubes (MWCNTs) dispersed onto a silicon substrate have been coated with diamond nanocrystals (DNC) and silicon carbide (SiC) from solid carbon and silicon sources exposed to H<sub>2</sub> activated by hot filament chemical vapor deposition (HFCVD) at around 190°C substrate temperature. MWCNT coating by DNC initiates during filament carburization process at 80°C substrate temperature under conventional HFCVD conditions. The hybrid nanocarbon material was analyzed by scanning electron microscopy, transmission electron microscopy, energy dispersive X-ray spectroscopy, electron energy loss spectroscopy, selected area electron diffraction, X-ray diffraction and Raman spectroscopy. The structure of the MWCNTs is preserved during coating and the smooth DNC/SiC coating is highly conformal. The average grain size is below 10 nm. The growth mechanism of DNC and SiC onto MWCNT surface is discussed.

## 1. Introduction

Hybrid nano-structured carbon materials such as carbon nanotubes (CNTs) coated by diamond nano-crystals (DNC) in a conformal manner or CNTs network connecting DNC agglomerates are scientifically and technologically attractive because of the potential possibility of combining the excellent structural, thermal, mechanical, chemical, optical and electronic properties of both carbon allotropes [1,2,3,4,5]. Particular combinations of CNT and diamond surfaces have been expected to form chemically and mechanically stable interfaces [2]. CNTs exhibit high tensile strength, radial elastic deformability, toughness together with unique electronic transport properties [6]. Nanocrystalline diamond (NCD) films display high hardness and stiffness, low coefficient of friction, exceptional chemical inertness, biocompatibility, high thermal conductivity, negative electron affinity with proper surface treatment and high transparency in a wide range of wavelength [7]. It has been speculated that the combination of CNT and DNC could give rise to materials with novel properties that could be used in a wide range of applications such as functional composite materials, field emission and other electronic devices, biodevices, wear-resistant coatings, thermal management of integrated circuits, electrical field shielding and micro- and nano-electromechanical systems (MEMS/NEMS) [1,2,3,4,5,8,9,10,11].

There are several methods for the synthesis of hybrid nano-structured carbon material consisting of DNC agglomerates connecting CNTs [8,10,12] but none of them have shown the conformal coating of CNTs by DNC. Sun et al. obtained DNC from multi-walled CNTs (MWCNTs) which were exposed during 10 hours to hydrogen plasma at a substrate temperature,  $T_s$ , of 727°C [13]. CNTs were partially converted into amorphous carbon (a-C) onto which diamond nano-particles nucleated. DNC diameter ranged from 5 to 30 nm and corresponding nucleation density was of  $\sim 10^{11}$  /cm<sup>2</sup>. No conformal coating was observed. If MWCNT plasma exposure duration was increased to 20 hours, DNC grew into diamond nanowires but diamond nucleation density was not increased significantly [14,15,16]. Shankar et al. used hot-filament chemical vapor deposition (HFCVD) to synthesize nanometer-sized diamond particles (2 to 20 nm) nucleating and growing radially outward on the surface of MWCNTs which were previously pre-dispersed onto a silicon substrate. They identified a small parametric window in the diamond growth space-phase (2-5 % CH<sub>4</sub> in H<sub>2</sub>) wherein the CNTs were not destroyed and wherein their structure

was partially preserved. Conformal coating was not achieved neither. In order to enhance nucleation density of diamond on CNTs, Shankar studied the effects of substrate temperature, precursor concentration, CNT film thickness and pressure on nucleation density of diamond on CNTs. The conditions for maximum diamond nucleation density were found to correspond to cases where the CNTs were almost completely etched away by atomic hydrogen, which would indicate a limitation to achieve higher diamond nucleation density by this method and therefore conformal coating [17]. Besides, CNTs have been used to enhance diamond nucleation on various substrate, in particular on substrates which neither dissolve carbon nor form carbide, such as copper [18]. However, to the knowledge of the authors, there is no report hitherto on any survival of CNTs upon subsequent diamond film growth.

Terranova et al. reported on the growth of single-walled CNTs (SWCNTs) bundles coated by DNCs in a conformal manner, at a high substrate temperature ( $T_s=900^\circ\text{C}$ ), in one step, by a modified HFCVD process [9]. SWCNTs bundles (diameter < 120 nm) were formed first, followed by NCD coating. The size of the diamond grains with well-defined crystalline facets was of 20-100 nm. However this method suffers from significant drawbacks. In particular, the substrate temperature is too high for the integration of the hybrid CNT/nano-diamond material with temperature sensitive substrate materials. It is prohibitive for low-cost mass production. Also, the size of the diamond grains may result in insufficient conformal coating of CNT bundles. Sub-10 nm diamond grains are desirable to achieve higher conformal degree. Later, Terranova et al., while exploring other preparation routes which would be suitable to be scaled up and adapted to the requirements of electronic industries, reported the coating by standard HFCVD process of SWCNTs bundles [11]. The SWCNTs layers were deposited on silicon substrate by drop casting of dispersions composed of purified materials and methanol. The coating of the SWCNT bundles by diamond was carried out by HFCVD exposure using a mixture of 1% of  $\text{CH}_4$  diluted in  $\text{H}_2$  as feeding gas.  $T_s$  was estimated to be  $630^\circ\text{C}$ . The SWCNTs bundles appeared uniformly coated by nano-grains, typically of the order of 10 nm according to author's statement. Low-magnification scanning electron microscopy (SEM) images published do not allow estimating average grain size. No transmission electron microscopy image was provided. Reflection high energy electron diffraction analysis revealed rings characteristic of diamond phase. No comment was done on possible presence of SiC, which may form under

those conditions, onto the CNT and substrate surface. Therefore, it is not clear whether diamond was obtained on the silicon substrate or on the SWCNT bundles surface. In any case, substrate temperature remains prohibitive for various applications whereby CNTs must be integrated with temperature sensitive substrate materials.

Similarly, conformal silicon carbide (SiC) coating onto CNTs is of great interest for improving chemical and physical properties of CNTs. For instance, for improving the thermo-oxidative stability of CNTs used as nano-reinforcements for metal, ceramic or polymer matrixes or for improving the electron emission stability of CNTs used in field emission devices [19,20]. Nanocrystalline SiC exhibits high elasticity, strength, chemical inertness, wide band gap, high electron mobility and thermal conductivity. However, up to now, conformal coating of SiC onto CNTs is performed at too high CNT temperature. MWCNTs (40-1000 nm outer diameter) were coated with a nanometer-sized SiC layer (~50 nm grains) by the reaction of SiO(g) and CO(g) at temperatures of 1150-1550°C in vacuum. [19]. More recently, the result was achieved with MWCNTs of 15 nm external diameter, using polycarbosilane as precursor, heated at ~1300°C under an inert atmosphere [20]. The temperature used in both processes is too high. It is highly desired to coat CNTs by SiC at lower CNT temperature. Also, the processes developed so far do not allow coating CNTs located on a substrate, which would be highly desirable for various applications such as electronic ones.

In conclusion, no method providing CNTs coated by DNC and/or SiC in a conformal manner at low temperature (below 200°C), which is suitable to be scaled up and adapted to the requirements of various industries such as the electronic industries, has been reported to date.

Our research team has been investigating NCD growth at low substrate temperature by HFCVD for its integration with temperature sensitive materials, such as polymers, in emerging nanotechnologies [21,22,23]. For this purpose and in an attempt to reach high growth rate at low substrate temperature, we have recently focused on the use of a solid carbon source etched by atomic H, instead of a conventional hydrocarbon gas precursor activated by HFCVD or microwave CVD (MWCVD). Such carbon solid source method was previously employed by various groups to grow CVD diamond films with higher conversion efficiency and growth rate in

comparison to conventional conditions; usually at  $T_S \geq 750^\circ\text{C}$  [24,25,26,27,28,29,30,31,32,33,34,35,36,37,38,39]. Yang et al. reported diamond synthesis at  $310 < T_S < 410^\circ\text{C}$  by MWCVD [35], but they did not provide any information on the film deposited on polytetrafluoroethylene (PTFE) which was used as substrate temperature indicator. A patent disclosed the synthesis of diamond by HFCVD on polyethylene terephthalate (PET) at  $T_S = 125^\circ\text{C}$  but there was no details on diamond structure, morphology and properties. The disclosure is based on a single Raman spectrum showing a sharp microcrystalline diamond peak [37]. Also, the set-up used in Ref. [37] is prone to graphite coating on filament which eliminates its catalytic effect and degrades film quality. Besides, solid carbon and silicon sources were used to grow nanocrystalline SiC films on Si substrate at  $T_S = 750^\circ\text{C}$  by HFCVD [40]. A solid graphite plate was used as the carbon source, and the silicon source came from the substrate itself. The only feeding gas into the system was  $\text{H}_2$ . This method is simple as compared to other CVD methods to produce SiC which involve a variety of gases; some of them being toxic and flammable such as silane and methyl silane. Recently we obtained NCD films composed of small grains ( $\sim 10$  nm and below), on various substrates, including copper, at  $T_S \sim 190^\circ\text{C}$  and high growth rate ( $> 3$   $\mu\text{m}/\text{h}$ ), by using a graphite substrate holder exposed to  $\text{H}_2$  activated by hot-filaments and without any substrate pre-treatment to enhance nucleation density as conventionally required, in particular for the substrates which neither dissolve carbon nor form carbide [41]. We showed that this method provides short induction time, high nucleation density, and high conversion efficiency and growth rate, even at such low substrate temperature [41]. We employed the method to successfully grow diamond on polyimide substrate with glass transition temperature of  $360^\circ\text{C}$  [41]. Also, by adding a silicon solid source, we elaborated nanocomposite films, containing diamond and SiC nanocrystals at  $T_S \sim 190^\circ\text{C}$  [41,42]. From those results and state of the art on CNTs coating, we hypothesized that this solid source method might be used to achieve high diamond and SiC nucleation density and highly conformal coating onto MWCNTs at low CNT and substrate temperature, before those ones get completely etched away by atomic hydrogen.

In this study, we present results on the investigation of MWCNTs conformally coated with DNC and SiC at low substrate temperature (below  $\sim 190^\circ\text{C}$ ) using solid carbon and silicon sources

exposed to  $H_2$  activated by HFCVD. Coating mechanism is discussed. The method is attractive for large scale production.

## 2. Experimental

(100) silicon (500-550  $\mu\text{m}$  thickness, 14 mm X 14 mm N/As type; from Nova Electronics Materials) and copper foils (99,9 % purity, 0.5 mm thickness, 14 mm diameter; from Goodfellow) were used as substrates. They were cleaned in acetone, rinsed in deionized water and dried in nitrogen at room temperature. Then, they were immersed in a solution of isoproponol containing MWCNTs, which were provided by Prof. Mauricio Terrones (Advanced Materials Department, IPICYT, Mexico). After 30 minutes of sonication under mild conditions (ultrasonic power of 60 W; frequency of 40 kHz), they were removed from the solution and dried under chemical hood atmospheric conditions. No effort was made to achieve high MWCNTs dispersion. The MWCNTs were obtained from the spray catalytic pyrolysis of toluene ( $\text{C}_7\text{H}_8$ ) and ferrocene ( $\text{FeCp}_2$ ) solutions at 800  $^\circ\text{C}$  using argon as carrier gas, as previously described in details [43]. 1 wt.% of EtOH in a  $\text{FeCp}_2$ - $\text{C}_7\text{H}_8$  solution containing 2.5 wt.% of  $\text{FeCp}_2$  was employed. High magnification SEM images were used to measure the dimensions of the tubes from an average of 80-100 measurements. Average diameter and length were estimated to be of around 55 nm and 300-400  $\mu\text{m}$ , respectively [43]. Iron content in MWCNT sample was estimated from thermogravimetric analysis to be below 6 wt.%. The ratio of the D band intensity on the G band intensity in Raman spectra taken at 514.5 nm was estimated to be of around 0.34016 and corresponded to the highest degree of crystallinity obtained for a series of MWCNT sample synthesized from different concentrations of EtOH and  $\text{FeCp}_2$  [43]. This conclusion was also confirmed by X-ray diffraction analysis [43].

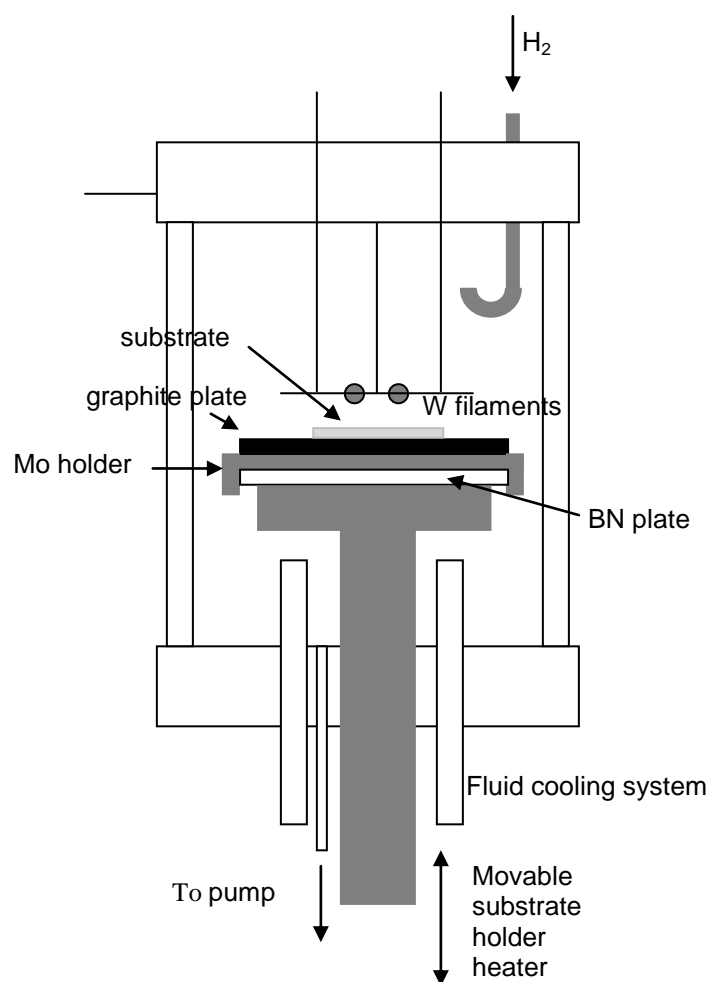


**FIG. 1.** Schematic of the HFCVD system.

A commercial HFCVD system (BWI 1000 model from Blue Wave Semiconductors) was used for synthesis (**FIG. 1**). The reactor is a 6 way cross stainless steel vacuum chamber. It is fluid cooled (15% water, 75% glycol, setting point of 18°C) with brazed copper tubing covered with Al foil. The reactor is equipped with a Mo filament cartridge that accommodates one to three 0.5 mm diameter straight W wires. Typically, two 5.7 cm length wires, 1 cm apart, are used. The substrates were placed on the movable and fluid-cooled 5 cm diameter stainless steel sample stage. On the latter were placed successively a BN plate, a Mo holder and a high-purity graphite plate (from Alfa Aesar), on top of which was located the substrate. A new graphite plate was used for each synthesis. High vacuum grease (70-90 wt. % polydimethylsiloxane, 7.0-13.0 wt. % silicon dioxide, 5.0-10.0 wt. % silicone metalloid complex; from Dow Corning ®) was used to maintain the substrate fixed on the graphite plate. The substrate temperature was estimated by a thermocouple (K-type; sheathed wires) located just below the surface of the Mo holder. A hole was drilled on the side of the Mo holder reaching its center. The thermocouple tip was inserted into the hole. Before synthesis, the HFCVD system was evacuated to below  $4 \times 10^{-4}$  mbar using a turbomolecular pump backed with a hydrocarbon oil pump. Ultra high purity (UHP) gases were introduced via a stainless steel tube located on top of the chamber. Gas flow was regulated by Omega mass flow controllers. The pressure, P, was regulated via an automatic valve located below the substrate holder. The filament temperature,  $T_F$ , was monitored with a two color pyrometer (M90R2 model from Mikron Infrared Inc). Before synthesis, the filament was carburized for 30 min in a mixture of 10 % of  $\text{CH}_4$  in  $\text{H}_2$ . The pressure and gas flow were of 10 Torr (13.3 mbar) and 50 sccm, respectively. The distance between the Mo holder and the filaments, d, was of ~41.6 mm. The current for both filaments was kept constant at 47 A.  $T_F$  was found to increase from 2000 to 2410°C during the first 26 min and then remained constant. After 30 min of carburization, the substrate temperature reached ~81°C. For synthesis,  $\text{H}_2$  was introduced into the chamber while  $\text{CH}_4$  was removed. The pressure and flow were kept constant at 10 Torr and 100 sccm, respectively. The filament current was raised and maintained at 55 A, which resulted in a filament temperature of 2550°C. The distance d was decreased to 9.8 mm. The resulting substrate temperature was of ~190°C. The MWCNTs were exposed to those conditions for 8 hours.

The surface morphology was investigated by scanning electron microscopy (SEM) using a JEOL JSM-7500F field emission scanning electron microscope. The structure was analyzed by transmission electron microscopy (TEM), energy dispersive X-ray analysis (EDX), electron energy loss spectroscopy (EELS) and selected area electron diffraction (SAED) using an energy filtered LEO-922 OMEGA microscope equipped with an Omega filter and EDAX Genesis 2000 microanalysis system (accelerating voltage of 200 kV). For this purpose, 3 nm thick holly carbon coated Cu grids were prepared by scratching the samples with a commercial diamond tip. X-ray diffraction (XRD) and Raman spectroscopy (RS) were also employed to examine the structure. The XRD measurements were taken on a Siemens D5000 diffractometer using a Cu K $\alpha$  line source ( $\lambda = 1.5405 \text{ \AA}$ ) in a  $\theta$ - $2\theta$  configuration. The Raman spectra were recorded with a triple monochromator (ISA J-Y Model T64000) using the 514.5 nm line of Ar laser and a  $\times 80$  objective. The probed area was of  $\sim 2 \mu\text{m}^2$ . A Renishaw InVia Reflex Spectrometer System with a stigmatic single pass spectrograph was also used for Raman analysis. In this case, the 488 nm line of an Ar ion laser and a  $\times 50$  objective were used. The laser power on the sample, and acquisition time were adjusted to obtain optimum signal without any sample modification. No visible damage and no change of the spectral shape during measurements have been observed. Silicon was used for peak position calibration.

### 3. Results and discussion

#### 3.1. Diamond coating

**FIG. 2** shows SEM micrographs of  $\sim 100$ - $200$  nm diameter and up to  $1\ \mu\text{m}$  in length, nanowires obtained from the silicon substrate region where MWCNTs were successively dispersed, were exposed to carburization and then to synthesis. The surface of those nanowires exhibits a highly conformal coating of sub- $10$  nm diameter grains (**FIG. 2B-D**).

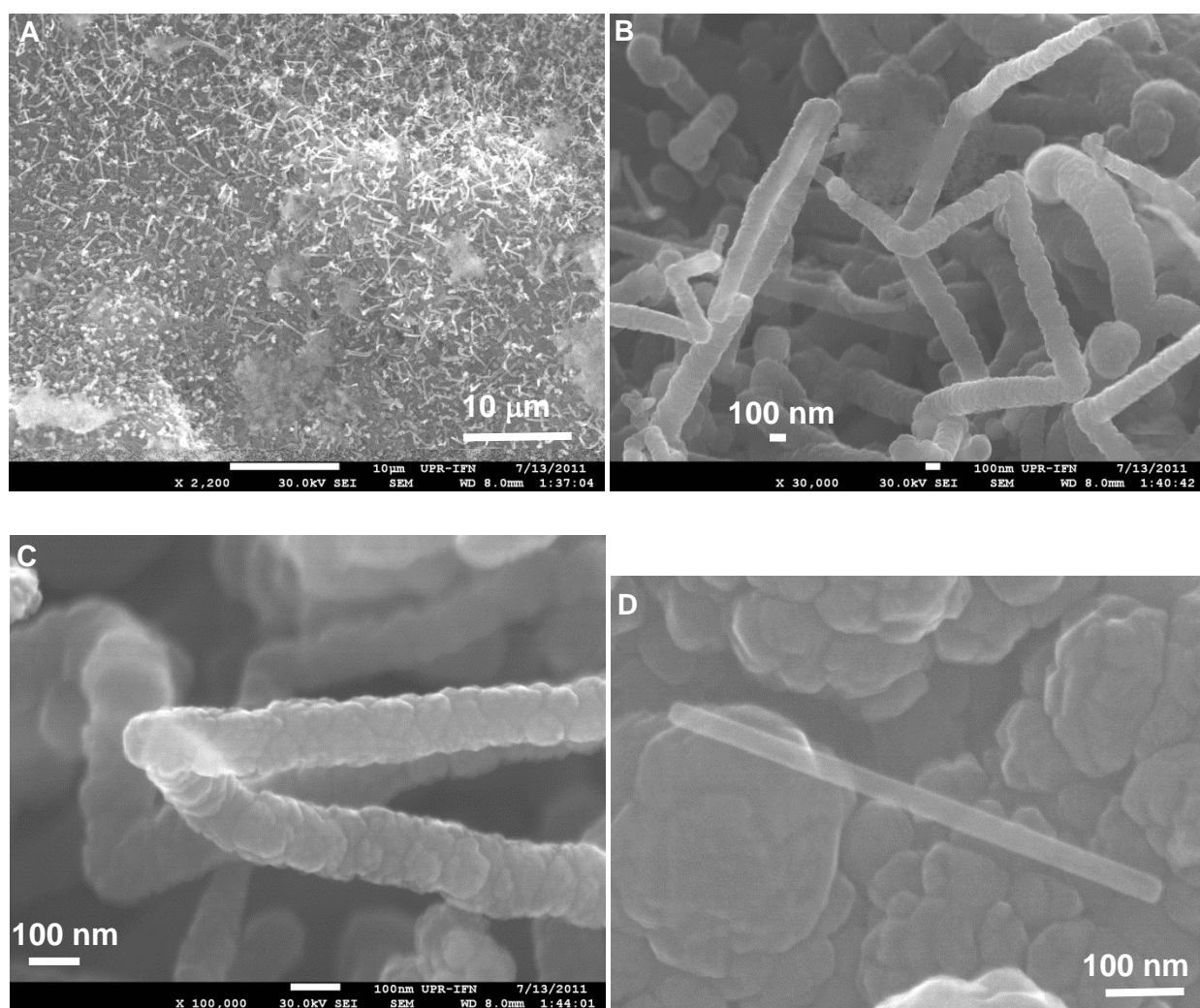


**FIG. 2.** SEM micrographs (different magnification) from the silicon substrate region where MWCNTs were successively dispersed, exposed to carburization and then to synthesis from solid C and Si sources (100 sccm  $\text{H}_2$ ,  $P=10$  Torr;  $d=9.8$  mm;  $T_F=2541^\circ\text{C}$ ; duration: 8 hours)

Nanowires coated in a conformal manner by nano-structured grains are observed (**A-C**). Uncoated MWCNTs are also detected (**D**).

**FIG. 3** presents TEM images of such nanowires. The dimension of the nanowires observed under TEM is consistent with the dimension of the nanowires observed under SEM. An extensive TEM investigation shows that the nanowires observed under SEM and under TEM are of the same nature. **FIG. 3A-B** reveal 100 nm diameter MWCNTs covered by faceted grains (white arrows) showing that MWCNTs survived HFCVD exposure. This will be further discussed in section 3.2. **FIG. 3D-F** show 150 nm diameter and 1  $\mu\text{m}$  length nanowire. Magnified TEM images reveal lattice fringes of nano-crystals of different orientation on the surface of the nanowires (**FIG. 3E-F**). The value estimated from **FIG. 3E** and from 7 planes (white arrow) is of 2.06  $\text{\AA}$ , as compared to the theoretical value of 2.059  $\text{\AA}$  corresponding to diamond  $\langle 111 \rangle$  lattice spacing. Therefore TEM images show the presence of MWCNTs with a conformal coating of sub 10-nm grains, some of them being diamond nano-crystals. Beside, Carbon *K-edge* EELS spectra obtained from coated MWCNTs (**FIG. 4**) are similar to EELS and NEXAFS spectra of NCD thin films [44]. The peak at  $\sim 284$  eV, from  $\text{C}1\text{s}-\pi^*$  transitions in  $\text{sp}^2\text{-C}$ , is not well defined and not well separated from the band centered at  $\sim 299$  eV, from  $\text{C}1\text{s}-\sigma^*$  transitions in  $\text{sp}^3\text{-C}$  and in  $\text{sp}^2\text{-C}$ , even though the spectra include the contribution from the Holly carbon grid and from MWCNTs. The characteristics of the  $\text{C}1\text{s}-\pi^*$  band suggest that a  $\text{sp}^3\text{-C}$  rich material covers MWCNTs. The deep at  $\sim 312$  eV is interpreted as the second band-gap of diamond [45]. These results strongly indicate that the coating on the surface of MWCNTs is made of a DNC. This is consistent with TEM observations.

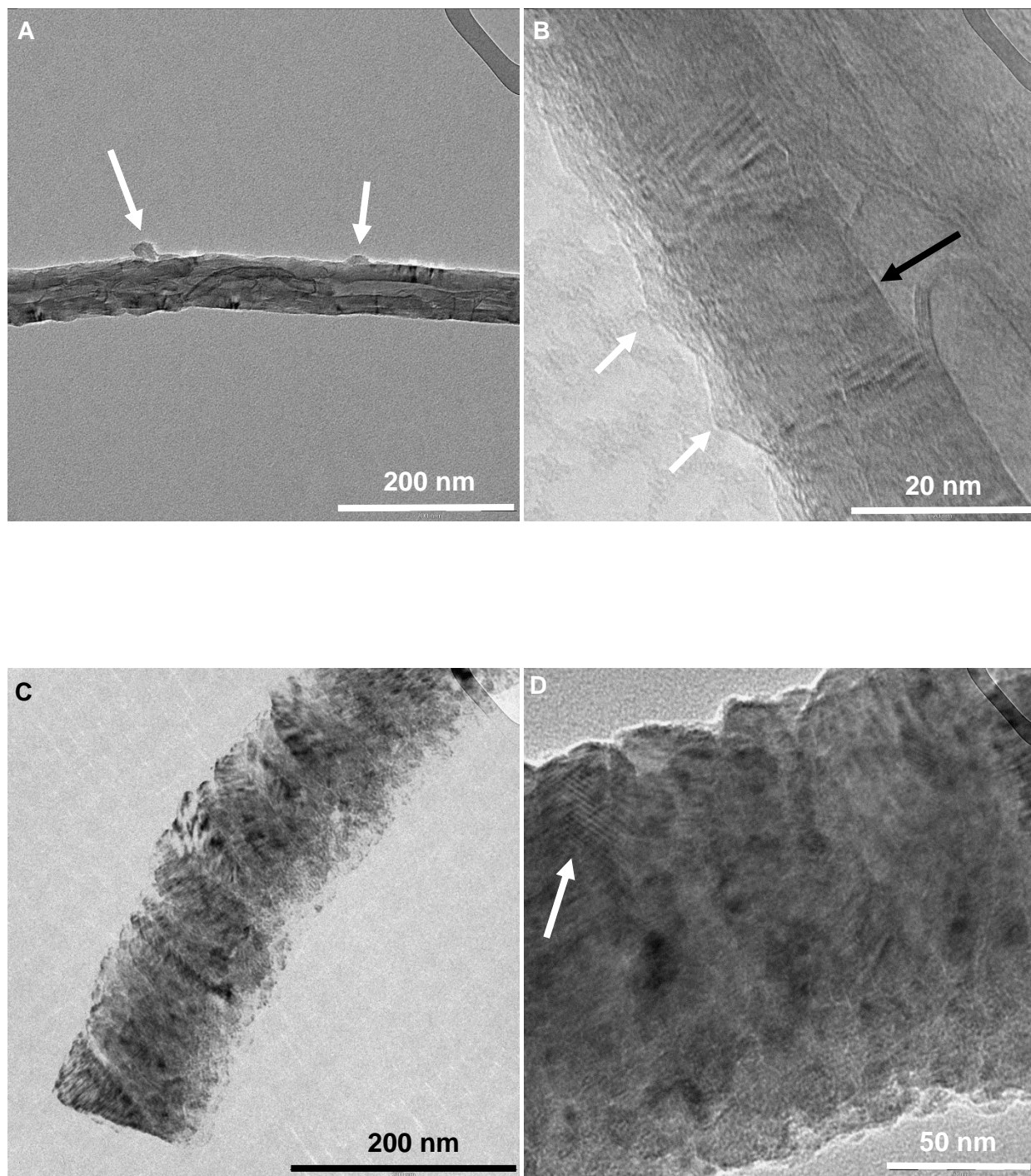


**FIG. 3.** TEM images of MWCNTs coated by nanostructured grains. Faceted grains are visible on the surface of the CNTs (white arrows) (**A-B**). The walls of MWCNTs are observed showing that the structure of MWCNTs is preserved during coating process of CNTs (black arrow) (**B**). (111) diamond lattice fringes are observed (white arrow) on the surface of the tubes (**D**).

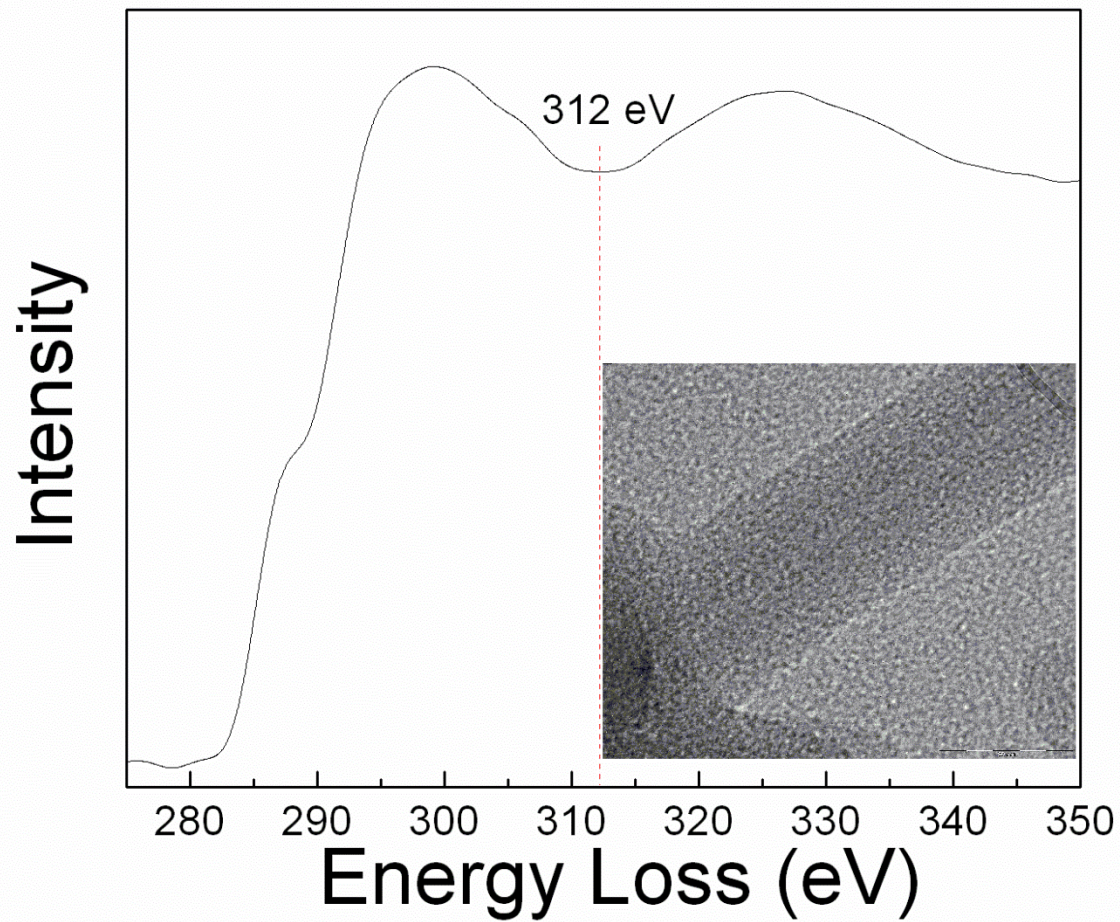
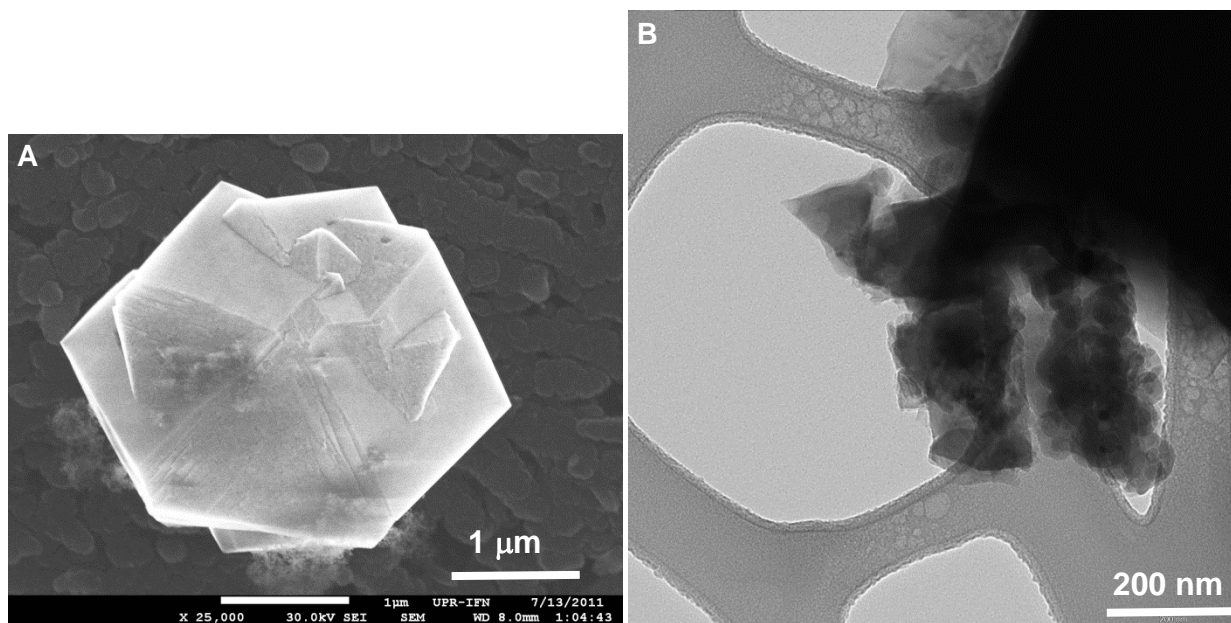


**FIG. 4.** Carbon K-edge spectrum of CNTs coated by diamond nano-crystals and SiC with a high conformal degree at low CNT and substrate temperature ( $\sim 190^\circ\text{C}$ ).

Also, this is consistent with other observations evidencing the presence of diamond in the samples:

1. In some region of the substrate free of MWCNTs, diamond micro- and nano-crystals are observed under SEM (**FIG. 5A**).
2. Thick agglomerates of faceted crystals are observed under TEM. Some of them exhibit a triangular shape; others a square shape (**FIG. 5B**). They are supposed to be DNCs.
3. Electron diffraction patterns obtained from extensive regions are characteristic of diamond. In some regions, patterns present (111), (220) and (311) diamond planes diffraction rings (**FIG. 5C**). In other region, the characteristic pattern of mono-crystalline diamond is obtained (**FIG. 5D**).
4. Carbon K-edge EELS spectra obtained from thick agglomerates are similar to typical EELS and NEXAFS spectra of NCD.
5. XRD diffractogram clearly shows diamond (111) diffraction peak (**FIG. 6**).

From our results, the presence of some amorphous carbon cannot be ruled out. Further structure analysis is required to clarify this point.



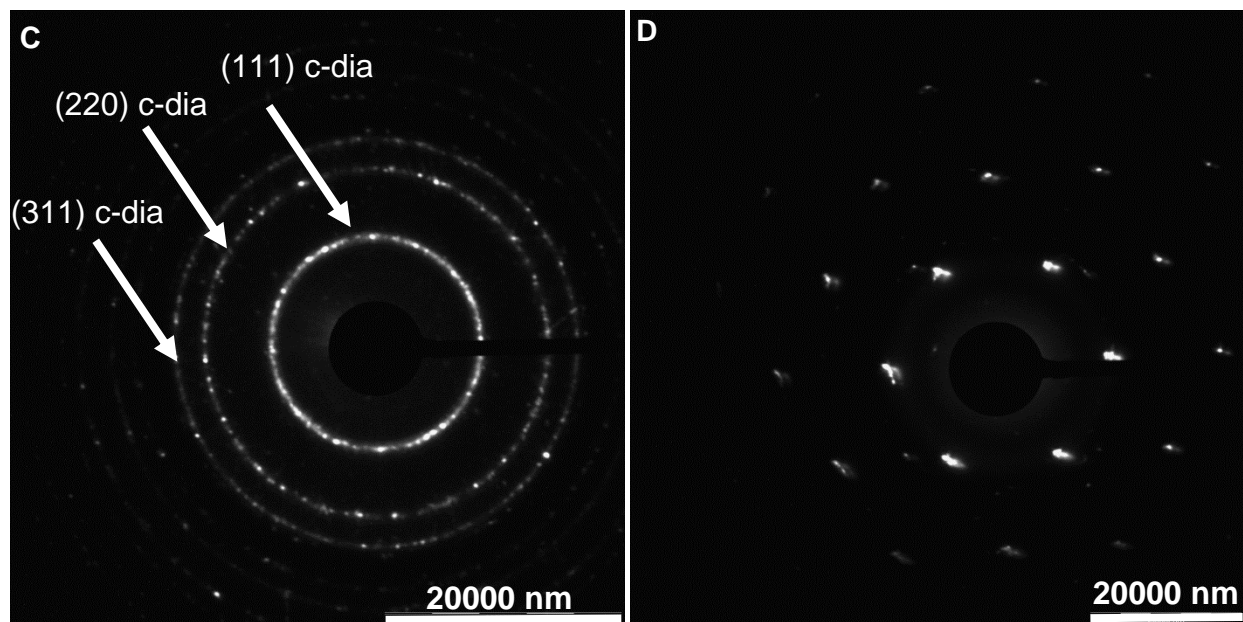


**FIG. 5.** Diamond crystals observed in region free of MWCNTs by SEM (A). Thick agglomerates of faceted crystals observed under TEM (B). Characteristic diamond Electron diffraction patterns obtained from extensive regions (C-D). In some regions, patterns present (111), (220) and (311) diamond planes diffraction rings (C). In other region, the characteristic pattern of monocrystalline diamond is obtained (D).

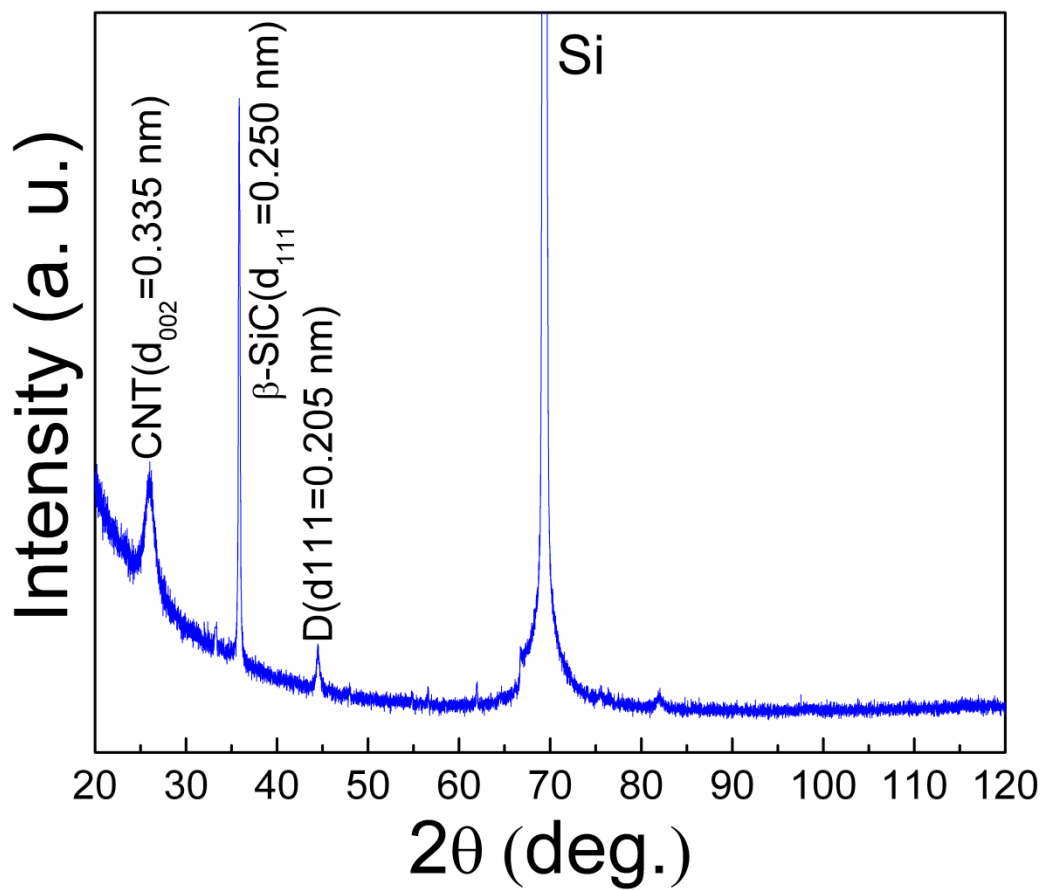


**FIG. 6.** X-ray diffraction pattern of a sample consisting of MWCNTs dispersed on a silicon substrate and exposed to carburization and then to 100 sccm H<sub>2</sub> flux in presence of solid carbon and silicon sources (P=10 Torr; d=9.8 mm; T<sub>F</sub>=2541°C; duration: 8 hours).

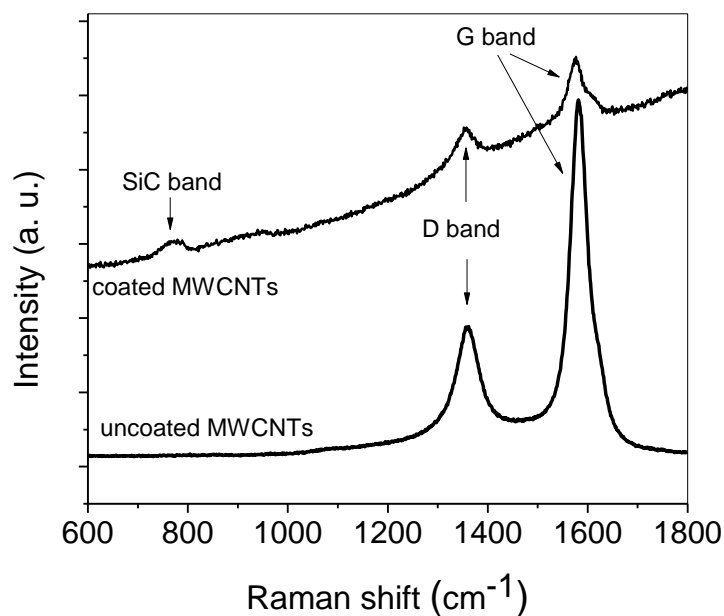
### 3.2. CNT survival under HFCVD exposure

As partially indicated in section 3.1, various results show that MWCNTs are not destroyed during the synthesis process, maintain their structure and that nanowires covered by diamond nanocrystals consist of MWCNTs on their center:

1. MWCNTs without any coating are observed on some SEM (**FIG. 2D**) and TEM images. Their diameters are within the range of diameters of the pristine MWCNTs (section 2) [43].
2. On some TEM images, as indicated in section 3.1, faceted crystals on the surface of MWCNTs are observed (**FIG. 3A-B**). In **FIG. 3B**, the MWCNT walls are clearly seen (black arrow).
3. Raman spectra of the region including coated MWCNTs (**FIG. 7**) exhibit characteristic MWCNT D and G bands. The low intensity of those bands, and the low relative intensity of the G band,  $I_G$ , with respect to the relative intensity of the D band,  $I_D$ , are compatible with the presence of a coating on the MWCNTs surface.  $I_D / I_G$  ratio of untreated MWCNTs is typically of  $\sim 0.26$ . It increases to  $\sim 0.38$  after sonication, and to  $\sim 0.79$  after coating treatment (**FIG. 7**).

It is worthwhile mentioning that, although the results show that some MWCNTs survived the processes, they do not prove that all of them survived nor that some did not suffer any modification. Further investigation is necessary to address this point.

A



B

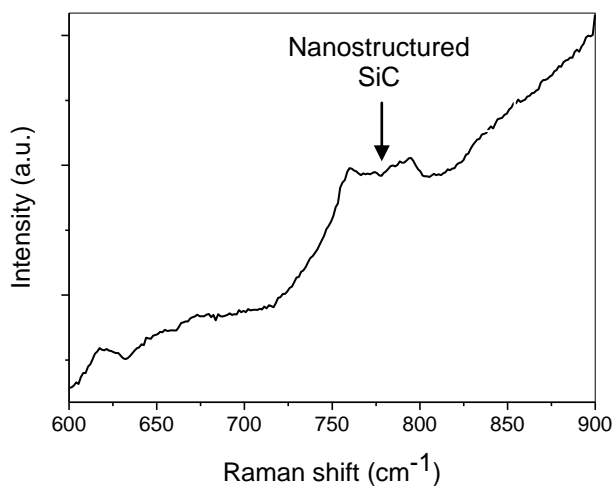


**FIG. 7.** Raman spectra taken at 488 nm of a sample consisting of MWCNTs dispersed on a silicon substrate and exposed to carburization and then to 100 sccm  $H_2$  flux in presence of solid carbon and silicon sources ( $P=10$  Torr;  $d=9.8$  mm;  $T_F=2541^\circ C$ ; duration: 8 hours): **(A)** MWCNTs region ; **(B)** MWCNTs and micro-crystalline diamond free region. Silicon First and Second order peaks are also observed in the spectra. Typical Raman spectrum of uncoated MWCNTs after sonication treatment is included in (A) for reference.

### 3.3. SiC coating

Various results strongly indicate that the MWCNTs are partially coated in a conformal manner with SiC grains entailing that the MWCNTs are conformally coated with a mixture of diamond nanocrystals and SiC grains. Those results are the followings:

1. EDX analysis performed under TEM, reveals, beside carbon, strong silicon content in the coated MWCNTs.
2. A peak at  $2\theta \sim 36^\circ$  corresponding to  $\beta$ -SiC (111) is observed in XRD diffraction pattern (**FIG. 6**).
3. Raman spectra of nanowires region show a broad and low relative intensity band at  $\sim 790 \text{ cm}^{-1}$ , corresponding to the transverse optical phonons of SiC (**FIG. 7A**). The broadness of the band is indicative of very short-range order [46].
4. TEM images of the nanowires obtained by the present method show some similarities with those reported for MWCNTs coated with a nanometer sized SiC layer by the reaction of SiO(g) and CO(g) at temperatures of 1150-1550 °C in vacuum [19]. In this later case, SiC granules, 20 to 200 nm in size, were observed.
5. In regions free of diamond microcrystals and MWCNTs, a nanostructured film of sub-10 nm grains is observed. XRD patterns (**FIG. 6**) and Raman spectra (**FIG. 7B**) suggest that this is nanostructured SiC. Apart from the Si first and second order Si peaks, a broad and low intensity band, from  $\sim 760$  to  $800 \text{ cm}^{-1}$ , from nanostructured SiC, is detected [46].

It is supposed that fast MWCNTs coating by SiC and diamond from fast etching of carbon and silicon solid sources by atomic hydrogen disable MWCNTs etching under further atomic H exposure. If CNTs are dispersed on copper substrates and if silicon grease is not used, MWCNTs are not observed but micro- and nano-crystalline diamond, as evidenced by SEM and Raman spectra. This is consistent with previous studies on the use of MWCNTs to enhance diamond growth (section 1). Also, when Si was used as substrate but without using silicon grease, CNTs coatings were not observed which indicates that silicon source is from the silicon grease.

### 3.4. Effect of carburization process

As before diamond synthesis, it is necessary to carburize the filaments and as there is no shutter between those ones and the substrates, we checked for any modification of the MWCNTs upon carburization. **FIG. 8** shows SEM micrographs of MWCNTs dispersed on a copper substrate after carburization in presence of a solid carbon source. In this case, silicon grease was not used. SEM micrographs reveal sub-10 nm nanometer grains on the surface of the MWCNTs. High charging effect under electron beam exposure suggests that the grains are insulating. Grains appear smaller and coating thinner than after diamond synthesis, which indicates that the coating process extends during the synthesis process. Compared to Raman spectra after synthesis (**FIG. 7**), Raman spectra after carburization show both, higher D and G relative intensity and  $I_G / I_D$  ratio. These observations confirm that MWCNTs are more altered during synthesis than during carburization process. EELS spectra and ED pattern exhibit similar characteristics than after synthesis. This indicates that the coating of MWCNTs by NCD initiates during carburization at very low temperature, around 80 °C. Similar observations were done without using solid carbon source during carburization. In conclusion MWCNTs coating initiates during carburization, with or without a solid carbon source (other than MWCNTs) at around 80°C. This is an interesting result since coating was so far achieved by conventional HFCVD at substrate temperature above 650°C [11].

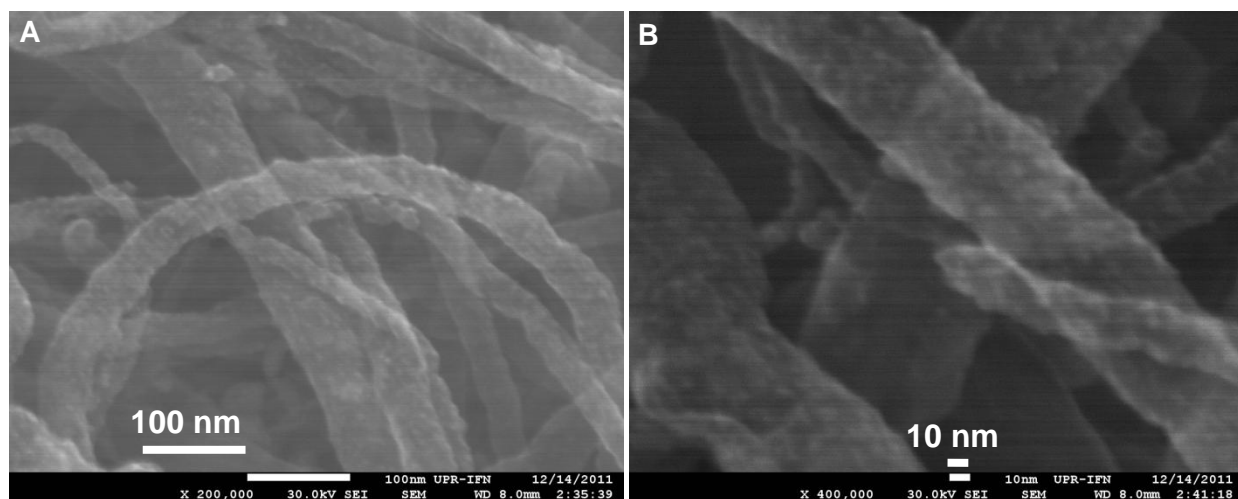


**FIG. 8.** SEM of MWCNTs after carburisation (without any silicon source).

### 3.5. Growth mechanism

The coating of MWCNTs by diamond nano-crystals and SiC under the present experimental conditions is tentatively and partially understood from several key factors as described below.

Firstly, as shown in section 3.4, MWCNTs coating initiates during carburization with or without any solid carbon source (other than MWCNTs) at very low substrate temperature (down to around 80°C) while using a high concentration of CH<sub>4</sub> in H<sub>2</sub> (10 %). During this process, MWCNTs are 41.6 mm away from the filaments so that they are exposed to mild HFCVD conditions as compared to standard HFCVD conditions using hydrocarbon precursor [10,11,17].

Secondly, during the carburization and synthesis, the substrate temperature is below 200°C. It is expected that, under the present experimental conditions and according to results reported on the etching of single-walled CNTs (SWCNTs) exposed to H<sub>2</sub> plasma [47], MWCNTs, which are less reactive than SWCNTs, survive H<sub>2</sub> plasma exposure.

Thirdly, the solid source HFCVD method used here for the synthesis is characterized by higher conversion efficiency as compared to conventional gas source HFCVD method, even at low substrate temperature [35,37,41]. According to previous studies [27,41], the growth of diamond from this method is believed to involve the following processes:

- (1) activation of hydrogen by the filaments to form atomic hydrogen and transport of hydrogen radicals to the graphite,
- (2) etching of graphite by atomic hydrogen and formation of hydrocarbon species,
- (3) transport of the hydrocarbon radicals and atomic hydrogen to the substrate and CNT surface to form diamond nano-crystals.

The growth of diamond from solid source is more effective than that from gas source, since in the first case, it has been possible to achieve higher nucleation density and to form continuous diamond films, without seeding pre-treatment, even on substrates which neither dissolve carbon nor form carbide such as copper [27,41]. It has been suggested that this is due to higher production of hydrocarbon radicals and higher proportion of hydrocarbon radicals taking part

into diamond growth when a solid source is used instead of a gas one. In conventional HFCVD, hydrocarbon radicals are formed only when hydrocarbon molecules have passed over the filament or reacted with atomic hydrogen [27]. Then only a small fraction of those radicals is deposited in the form of diamond because of the long-range transport required in the gas phase and the short life time of the radicals participating in the diamond formation process [26]. On the other hand, in solid carbon source method, the reaction products between atomic hydrogen and graphite are predominantly hydrocarbon radicals and a high fraction of those radicals contribute to diamond growth. It has also been speculated that, in solid carbon method, the increase in nucleation may be due to the formation of some short-lived species, which nature has not been determined, as etching products of hydrogen and graphite [27]. The effective production of hydrocarbon radicals from graphite etching is best used for diamond growth when the graphite source is close to the substrate as discussed below. Higher concentration of hydrocarbon radicals usually results in higher diamond growth rate and higher second nucleation rates of diamond, which has been confirmed by placing the substrate closer to the filament in conventional HFCVD process [35].

One remarkable result obtained here is that, while graphite is efficiently etched by atomic hydrogen, MWCNTs, which are located closer to the filaments than the graphite plate, can withstand atomic hydrogen exposure. As the presence of SiC on the surface of the MWCNTs was evidenced in section 3.3., it is tentatively supposed that fast MWCNTs coating by SiC and diamond from fast etching of C and Si solid sources by atomic hydrogen, located near the substrate, disable MWCNTs etching under further atomic H exposure. Further investigation is necessary to clarify this point.

Fourthly, in our case, the graphite plate is located just below the substrate so that there is a short distance between the solid source and the substrate. The concentration of the activated hydrocarbon radicals is highest around the graphite plate and decreases away from the plate. Therefore there is higher concentration of hydrocarbon radicals near the substrate than near the filaments. The reverse situation occurs in conventional HFCVD as indicated above. In the case of solid carbon source, it was shown that it is necessary to place the substrate close to the graphite plate to achieve high diamond growth rate [35]. Higher concentration of activated transitional hydrocarbon radicals around the substrate is believed to contribute to higher diamond

quality, higher growth rate and finer grain size of diamond films in this graphite etching process [35]. Another advantage of placing the graphite plate near the substrate is that the filament might not be coated by graphite. It is known that HFCVD process is limited in growth rate because high concentration of hydrocarbon for the high growth rate leads to graphite coating on filament. Once the filament is coated by graphite, the catalytic effect filament vanishes and the quality of films is degraded [33]. By placing the graphite below the substrate, it is possible to fully utilize the catalytic effect of the tungsten filaments while an appreciable amount of carbon-rich gas is supplied to the substrate through etching of the graphite plate by hydrogen radicals [33].

Fifthly, the presence of an additional silicon source (other than that the Si substrate) is paramount to achieve MWCNTs coating in the present synthesis conditions. As indicated in section 3.3., if CNTs are dispersed on copper substrates and if silicon grease is not used, or if Si is used as substrate but without using silicon grease, CNTs coatings were not observed, but micro and nano-crystalline diamond. This strongly indicates that MWCNTs etching is disabled by diamond and SiC coating onto the surface of the MWCNTs. Further study is necessary to characterize the evolution of the structure of the hybrid materials during carburization and coating processes to determine precise growth mechanisms.

In conclusion, a new coating pathway has been developed to coat CNTs with diamond nano-crystals and SiC with high conformal degree at low CNT and substrate temperature, down to  $\sim 190^{\circ}\text{C}$ . The method may be suitable for mass-production. The hybrid nanocarbon material elaborated from this method may be further investigated to be used in functional and thermo-resistant composite materials and as stable emitters in field emission devices [48].

#### **4. Conclusion**

A new coating pathway has been developed to obtain CNTs coated with diamond nano-crystals and SiC with high conformal degree at low CNT and substrate temperature, down to  $\sim 190^{\circ}\text{C}$ . The synthesis of such hybrid nanocarbon material was achieved, via the exposure of CNTs dispersed on a silicon substrate maintained at  $\sim 190^{\circ}\text{C}$ , solid carbon and silicon sources to pure  $\text{H}_2$  activated by HFCVD. The structure of the MWCNTs is preserved and the coating is highly

conformal. The average size of the grains is below 10 nm. Nucleation was shown to initiate during carburization from a high content of  $\text{CH}_4$  in  $\text{H}_2$  at substrate temperature below  $80^\circ\text{C}$ . The growth of diamond nano-crystals and SiC onto the surface of CNTs in the present experimental conditions was discussed in terms of fast and effective etching of graphite and silicon source near the CNTs and deposition of C and Si. It is supposed that fast MWCNTs coating by SiC and diamond from fast etching of carbon and silicon solid sources by atomic hydrogen disable MWCNTs etching under further atomic hydrogen exposure. The hybrid nanocarbon material elaborated from this method may be further investigated to be used in functional and thermo-resistant composite materials and as stable emitters in field emission devices

## Acknowledgements

This research was partially funded by the Minister of Higher Education, Science and Technology, MESCYT, of the Dominican Republic (2007 and 2008 FONDOCYT programs; Grant Number 2008-1-B3-066). The authors wish to gratefully acknowledge the use of research facilities at the University of Puerto Rico, San Juan, Río Piedras Campus: Raman spectroscopy (R. Katiyar, W. Pérez), SEM (O. Resto, K. Perez), XRD (E. Resto), XPS (C. Cabrera, E. Fachini, N. Rivera). Carbon nanotubes were provided by Prof. Mauricio Terrones, Material Division, Pennsylvania State University. F.P. greatly acknowledges MESCYT for its strong support and PUCMM, for administrative, financial and technical support (Mgr. A. Nuñez Collado, S. González, I. Adames, M. Baez

---

## References

- [1] A.S. Barnard in *Ultrananocrystalline Diamond: Synthesis, Properties, and Applications*, O.A. Shenderova, D.M. Gruen, William Andrew Publishing, 2006, p146-147.
- [2] O.A. Shenderova, D. Areshkin, D.W. Brenner, Carbon based nanostructures: diamond clusters structured with nanotubes, *Mater. Res.* 6, 11-17 (2003).
- [3] O.A. Shenderova, D. Areshkin, D.W. Brenner, Bonding and Stability of Hybrid Diamond/Nanotube Structures, *Mol. Simulat.*, 29, 259-268 (2003).
- [4] A.S. Barnard, M.L. Terranova, M. Rossi, Density Functional Study of H-Induced Defects as Nucleation Sites in Hybrid Carbon Nanomaterials, *Chem. Mater.* 17, 527-535 (2005).
- [5] A.R. Muniz, T. Singh, E.S. Aydil, D. Maroudas, Analysis of diamond nanocrystal formation from multiwalled carbon nanotubes, *Phys. Rev. B* 80, 144105-144117 (2009).
- [6] M. S. Dresselhaus, G. Dresselhaus, and P. Avouris, *Carbon nanotubes: synthesis, structure, properties, and applications*. Berlin; New York: Springer-Verlag, 2001.
- [7] J.E. Butler, A.V. Sumant, The CVD of Nanodiamond Materials, *Chem. Vap. Deposition* 14, 145-160 (2008).
- [8] X. Xiao, J.W. Elam, S. Trasobares, O. Auciello, and J.A. Carlisle., Synthesis of a Self-Assembled Hybrid of Ultrananocrystalline Diamond and Carbon Nanotubes, *Adv. Mater.*, 17, 1496-1500 (2005).

- 
- [9] M.L. Terranova, S. Orlanducci, A. Fiori, E. Tamburri, V. Sessa, Controlled Evolution of Carbon Nanotubes Coated by Nanodiamond: the Realization of a New Class of Hybrid Nanomaterials, *Chem. Mater.* 17, 3214-3220 (2005).
- [10] Nagraj Shankar, Nick G. Glumac, Min-Feng Yu, S.P. Vanka, Growth of nanodiamond/carbon-nanotube composites with hot filament chemical vapor deposition, *Diamond Relat. Mater.*, 17, 79-83 (2008).
- [11] V. Guglielmotti, S. Chieppa, S. Orlanducci, E. Tamburri, F. Toschi, M. L. Terranova, M. Rossi, Carbon nanotube/nanodiamond structures: An innovative concept for stable and ready-to-start electron emitters, *Appl. Phys. Lett.* 95, 222113-222114 (2009).
- [12] X. Xiao, J.A. Carlisle, O. Auciello, J.W. Elam, D.M. Gruen, Synthesis of a Self Assembled Hybrid of Ultrananocrystalline Diamond and Carbon Nanotubes, US Patent No. 0222850 A1 (2006).
- [13] L. T. Sun, J. L. Gong, Z. Y. Zhu, D. Z. Zhu, S. X. He, and Z. X. Wang, Nanocrystalline diamond from carbon nanotubes, *Appl. Phys. Lett.* 84, 2901-2904 (2004).
- [14] L. Sun, J. Gong, D. Zhu, Z. Zhu, S. He, Diamond Nanorods from Carbon Nanotubes, *Adv. Mater.* 16, 1849-1853 (2004).
- [15] L.T. Sun, J.L. Gong, Z.Y. Zhu, D.Z. Zhu, Z.X. Wang, W. Zhang, J.G. Hu, Q.T. Li, Synthesis and characterization of diamond nanowires from carbon nanotubes *Diamond Relat. Mater* 14, 749-752 (2005).
- [16] J. L. Gong, L. T. Sun, D. Z. Zhu, Z. Y. Zhu, S. X. He, T. Yue and Z. X. Wang, *Int. J. Nanoscience*, 5, 307 (2006).
- [17] Nagraj Shankar, PhD dissertation, University of Illinois at Urbana-Champaign, 2004.
- [18] Ya-Qi Hou, Da-Ming Zhuang, Gong Zhang, Min-Sheng Wu, Jia-Jun Liu, Diamond Nanorods from Carbon Nanotubes by Hydrogen Plasma Treatment, *Appl. Surf. Sci.* 185, 303-313 (2002.)
- [19] Y. Morisada, Y. Miyamoto, SiC-coated carbon nanotubes and their application as reinforcements for cemented carbides, *Materials Science and Engineering A* 381, 57-61 (2004).
- [20] R.K. Gupta, R. Mishra, K. Mukhopadhyay, R.K. Tiwari, A. Ranjan, A.K. Saxena, A New Technique for Coating Silicon Carbide Onto Carbon Nanotubes Using a Polycarbosilane Precursor, *Silicon* 1,125-129 (2009).

- 
- [21] F. Piazza, J.A. González, R. Velázquez, J. De Jesús, S.A. Rosario, G. Morell, Diamond film synthesis at low temperature, *Diamond Relat. Mater.*, 15, 109-116 (2006)
- [22] F. Piazza, G. Morell, Synthesis of diamond at sub 300 °C substrate temperature, *Diamond Relat. Mater.*, 16, 1950-1957 (2007).
- [23] F. Piazza, F. Solá, O. Resto, L.F. Fonseca, G. Morell, Synthesis of diamond nanocrystals on polyimide film, *Diamond Relat. Mater.*, 18, 113-116 (2009).
- [24] M.C. Salvadori, J.W. Ager, I.G. Brown, K.M. Krishnan, Diamond synthesis by microwave plasma chemical vapor deposition using graphite as the carbon source, *Appl. Phys. Lett.* 59, 2386-2389 (1991).
- [25] L. Chow, H. Wang, S. Kleckley, A. Schulte, Diamond nucleation on graphite substrate using a pure hydrogen feed, *Solid State Comm.* 93, 999-1002 (1995).
- [26] S. Ismat Shah, D.J. Walls, Plasma assisted conversion of carbon fibers to diamond, *Appl. Phys. Lett.* 67, 3355 (1995)
- [27] H.K. Woo, S.T. Lee, C.S. Lee, I. Bello, Y.W. Lam, Diamond films grown by hot filament chemical vapor deposition from a solid carbon source, *J. Vac. Sci. Technol. A* 15, 2988-2993 (1997).
- [28] H.K. Woo, C.S. Lee, I. Bello, S.T. Lee, Oriented diamond growth on silicon (111) using a solid carbon source, *J. Appl. Phys.* 83, 4187-4193 (1998).
- [29] L.L. Regel, W.R. Wilcox, Selective Patterned Deposition of Diamond using a New Technique, *J. Mat. Sci. Lett.* 18, 427-430 (1999).
- [30] L.L. Regel, W.R. Wilcox, Deposition of diamond on graphite and carbon felt from graphite heated in hydrogen at low pressure, *J. Mat. Sci. Lett.* 19, 455-457 (2000).
- [31] L.L. Regel, W.R. Wilcox, Diamond film deposition by chemical vapor transport, *Acta Astronautica* 48, 129-144 (2001).
- [32] H. Liu, C. Wang, C. Gao, Y. Han, J. Luo, G. Zou, C. Wen, Diamond films grown on seeded substrates by hot-filament chemical vapour deposition with H<sub>2</sub> as the only feeding gas, *J. Phys.: Condens. Matter* 14, 10969-10972 (2002).
- [33] S.D. Shin, N.M. Hwang, D.Y. Kim, High rate of diamond deposition through graphite etching in a hot filament CVD reactor, *Diamond Relat. Mater.* 11, 1337-1343 (2002).
- [34] Q. Yang, W. Chen, C. Xiao, A. Hirose, M. Bradley, Elongation of arrays of amorphous carbon tubes, *Carbon* 43, 2618-2621 (2005).

- 
- [35] Q. Yang, W. Chen, C. Xiao, R. Sammynaiken, A. Hirose, Synthesis of diamond films and nanotips through graphite etching, *Carbon* 43, 748-754 (2005).
- [36] Q. Yang, W. Chen, C. Xiao, A. Hirose, R. Sammynaiken, Simultaneous growth of well-aligned diamond and graphitic carbon nanostructures through graphite etching, *Diamond Relat. Mater.* 14, 1683-1687 (2005).
- [37] L. Regel, A.D. Cropper, A Method for Manufacturing Low Temperature Diamond Coatings, US Patent No. 7,118,782 B2 (2006).
- [38] Q. Yang, S. Yang, C. Xiao, A. Hirose, Transformation of carbon nanotubes to diamond in microwave hydrogen plasma, *Mater. Lett.* 61, 2208-2211 (2007).
- [39] X. Lu, Q. Yang, C. Xiao, A. Hirose, Effects of hydrogen flow rate on the growth and field electron emission characteristics of diamond thin films synthesized through graphite etching, *Diamond Relat. Mater.* 16, 1623-1627 (2007).
- [40] H.K. Woo, C.S. Lee, I. Bello, S.T. Lee, Growth of epitaxial  $\beta$ -SiC films on silicon using solid graphite and silicon sources, *Diamond and Related Materials* 8, 1737-1740 (1999).
- [41] F. Piazza, J. Beltran Huarac G. Paredes, G. Morell, submitted.
- [42] F. Piazza, J. Beltran Huarac, G. Paredes, M. Ahmadi, G. Morell, M. Guinel, in preparation.
- [43] A. Botello-Méndez, J. Campos-Delgado, A. Morelos-Gómez, J.M. Romero-Herrera, A.G. Rodríguez, H. Vavarro, M.A. Vidal, H. Terrones, M. Terrones, Controlling the dimensions, reactivity and crystallinity of multiwalled carbon nanotubes using low ethanol concentrations, *Chemical Phys. Lett.* 453, 55-61 (2008).
- [44] X. Xiao, J. Birell, J.E. Jerbi, O. Auciello, J.A. Carlisle, Low temperature growth of ultrananocrystalline diamond, *J. Appl. Phys.* 96, 2232-2240 (2004).
- [45] A. Laikhtman, I. Gouzman, A. Hoffman, G. Comtet, L. Hellner, G. Dujardin, Sensitivity of near-edge x-ray absorption fine structure spectroscopy to ion beam damage in diamond films, *J. Appl. Phys.* 86, 4192-4199 (1999).
- [46] S. Klein, R. Carius, F. Finger, L. Houben, Low substrate temperature deposition of crystalline SiC using HWCVD, *Thin Solid Films* 501, 169-172 (2006).
- [47] G. Zhang, P. Qi, X. Wang, Y. Lu, D. Mann, X. Li, and H. Dai, Hydrogenation and Hydrocarbonation and Etching of Single-Walled Carbon Nanotubes, *J. Am. Chem. Soc.* 128, 6026-6027 (2006).
- [48] F. Piazza, Carbon Nanotubes Conformally Coated With Diamond Nanocrystals or Silicon

---

Carbide, Methods of Making the Same and Their Use, U.S. Utility Patent Application No. 14/079,546; International Patent Application No. PCT/US2013/069934; Taiwanese Patent Application No.102141512.